RESEARCH ARTICLE

Serum nuclear magnetic resonance metabolomics analysis of human metastatic colorectal cancer: Biomarkers and pathway analysis

Ana Isabel Tristán[1] | Encarnación González-Flores[2,3] | Ana del Mar Salmerón[1] |
Ana Cristina Abreu[1] | Octavio Caba[2,4,5] | Cristina Jiménez-Luna[2,4] |
Consolación Melguizo[2,4,5] | José Prados[2,4,5] | Ignacio Fernández[1]

[1]Department of Chemistry and Physics, Research Centre CIAIMBITAL, University of Almería, Almería, Spain

[2]Instituto de Investigación Biosanitaria de Granada (ibs. GRANADA), Granada, Spain

[3]Medical Oncology Service, Virgen de las Nieves Hospital, Granada, Spain

[4]Institute of Biopathology and Regenerative Medicine (IBIMER), Center of Biomedical Research (CIBM), University of Granada, Granada, Spain

[5]Department of Anatomy and Embryology, Faculty of Medicine, University of Granada, Granada, Spain

Correspondence
José Prados, Department of Anatomy and Embryology, Faculty of Medicine, University of Granada, 18071 Granada, Spain.
Email: jcprados@ugr.es
Ignacio Fernández, Department of Chemistry and Physics, Research Centre CIAIMBITAL, University of Almería, Ctra. Sacramento, s/n, 04120, Almería, Spain.
Email: ifernan@ual.es

Funding information
Junta de Andalucía, Grant/Award Numbers: 102C2000004, UAL2020-AGR-B1781, P20_01041; Gobierno de España, Grant/Award Numbers: PDC2021–121248-I00, PLEC2021–007774; Instituto de Salud Carlos III (ISCIII), Grant/Award Number: PI19/01478; CTS-107 and FQM-376 groups

Abstract

We describe the use of nuclear magnetic resonance metabolomics to analyze blood serum samples from healthy individuals (n = 26) and those with metastatic colorectal cancer (CRC; n = 57). The assessment, employing both linear and nonlinear multivariate data analysis techniques, revealed specific metabolite changes associated with metastatic CRC, including increased levels of lactate, glutamate, and pyruvate, and decreased levels of certain amino acids and total fatty acids. Biomarker ratios such as glutamate-to-glutamine and pyruvate-to-alanine were also found to be related to CRC. The study also found that glutamate was linked to progression-free survival and that both glutamate and 3-hydroxybutyrate were risk factors for metastatic CRC. Additionally, gas chromatography coupled to flame-ionization detection was utilized to analyze the fatty acid profile and pathway analysis was performed on the profiled metabolites to understand the metabolic processes involved in CRC. A correlation was also found between the presence of certain metabolites in the blood of CRC patients and certain clinical features.

Abbreviations: CRC, colorectal cancer; NMR, nuclear magnetic resonance; GC-FID, gas chromatography coupled to flame-ionization detector; FOBT, fecal occult blood test; CEA, carcinoembryonic antigen; CA19-9, carbohydrate antigen 19-9; MS, mass spectrometry; MVDA, multivariate date analyses; SD, standard deviation; TSP, 3-(trimethylsilyl)propionic-2,2,3,3-d_4 acid; TOCSY, total correlation spectroscopy; HMBC, heteronuclear multiple bonds coherence; PCA, principal component analysis; OPLS-DA, orthogonal projections to latent structures discriminant analysis; CV-ANOVA, cross validated analysis of variance; RF, random forest; MDA, mean decrease in accuracy; OOB, out-of-bag; AUROC, area under the receiver operating characteristics; PLS-DA, partial least squares discriminant analysis; SVM, support vector machine; ROC, receiver operating characteristics; MCCV, Monte-Carlo cross validation; AUC, area under the curve; FDR, false discovery rate; AIC, Akaike information criterion; FA, fatty acid; UFA, unsaturated fatty acid; PUFA, polyunsaturated fatty acid; 3HB, 3-hydroxybutyrate; Ala, alanine; Chol, choline; Cit, citrate; Cr, creatine; GPC, glycerophosphocholine; Glc, glucose; Gln, glutamine; Glu, glutamate; Glyc, glycerol; His, histidine; Ile, isoleucine; Lac, lactate; Leu, leucine; Lys, lysine; NAGP, N-acetylglycoproteins; Phe, phenylalanine; Pyr, pyruvate; Trp, tryptophan; Tyr, tyrosine; Val, valine; VIP, variable importance in projection; GGR, glutamate-to-glutamine; PAR, pyruvate-to-alanine.

1 | INTRODUCTION

Colorectal cancer (CRC), the third type of cancer with the highest incidence worldwide and the second with the highest mortality, has created and still creates personal, familial, and economic costs for the health system and society as a whole.[1–3] In fact, it is estimated that, by 2035, CRC mortality will increase by more than 60.0%.[4] Primary prevention remains the key strategy to reduce its high mortality and is based on screening programs for early detection (i.e., colonoscopy, fecal occult blood test, etc.).[5,6] However, despite this preventive activity, approximately 20%–25% of patients already present with metastases at disease onset, while 50% of patients will eventually develop metastases,[7,8] directly resulting in a 5-year overall survival rate lower than 15%.[9] It is therefore necessary to develop a suitable method that is able to find new biomarkers for CRC diagnosis and prognosis, including the metastatic stage, that will help in the understanding of the function and dynamics of these discriminative metabolites within, for instance, gut microbiota, which has proven to be interplayed with the pathogenesis and/or progression of chronic non-communicable diseases, including cancer.[10] Glycoproteins such as serum carcinoembryonic antigen (CEA) or cell-to-cell recognition oligosaccharides such as carbohydrate antigen 19–9 (CA19–9) are well-known biomarkers for predicting different types of cancer, including CRC, although they have a very low overall success rate and accuracy.[11] Currently, the liquid biopsy[12] is widely assayed to determine novel diagnosis and prognosis of CRC biomarkers that include DNA, miRNA, lncRNA, and ctDNA, among others.[13–16] In this broad omic approach, the detection of metabolites in peripheral blood is a powerful and sensitive methodology that aims to improve CRC screening by defining metabolomic patterns, using all the clinical management benefits that an advanced diagnosis presumes in this type of pathology. In this area of metabolomics, Martín-Blázquez et al. have recently identified a molecular signature that is able to discriminate between patients with and without CRC, illustrating the potential of this approach to contribute new insights regarding the molecular mechanism and signaling pathways of metastatic CRC.[17]

Metabolomics, as already mentioned, is the systematic study of chemical fingerprints in biological systems, that unravels the presence and concentration of these metabolites in many tissues, including body fluids. This relatively young omics science, along with nuclear magnetic resonance (NMR), has recently been used in cancer diagnosis,[5,18,19] leading to the identification of biomarkers that differentiate diseased patients from healthy individuals or those with benign tumors. Previous research studies have employed intact tumor tissue,[20] fecal extracts,[21] and blood serum[5,22] as matrices to develop metabolomics studies. The use of serum samples is especially recognized, as long as does not require endoscopic treatment.[23] Nowadays, there are some examples of the use of metabolomics in developmental therapies.[24] Biomarkers are being applied to identify therapeutic targets, as well as to determine the action mechanism of some drugs, and even to monitor the response of given treatments.[25] In parallel, NMR has been increasingly applied in metabolomics studies, because it constitutes a quantitative and nondestructive technique that is able to determine unknown structures or metabolites in a fast and reproducible way.[26] As an advantage over other spectrometric techniques such as mass spectrometry (MS), NMR requires almost no sample preparation, which makes it especially suitable for biomedicine and clinical assays such as studying biological biofluids like blood, urine, cerebrospinal fluid, or tissues, without the need for extensive sample preparation or purification.[20,27] We have recently revised the published investigations dedicated to the research of metabolic changes produced in blood serum samples of CRC patients, mainly involving NMR alone and/or in combination with other analytical platforms.[26] Most of these studies agree on the role of metabolites involved in glycolysis because these appear to be highly boosted in carcinogenic samples, together with alterations in the amino acids content, the metabolism of glycerolipids and fatty acids.[26]

In the present contribution, we have developed a complete nontargeted metabolomics study using NMR coupled to multivariate data analyses (MVDA) to find differences in the blood serum metabolic profiles between metastatic CRC patients (n = 57; with different locations of the tumor) and healthy controls (n = 26). The aim of the current study was to identify potential serum biomarkers associated with metastatic CRC, understand the specific metabolic routes involved in the function and dynamics of CRC, then combine these for predicting and revealing disease in patients.

2 | MATERIALS AND METHODS

2.1 | Patients' characteristics

The clinical parameters of metastatic CRC patients (n = 57) and healthy controls (n = 26) who were included in the study are summarized in Table 1.

At the time of biomarker sampling, all patients had at least one radiologically visible metastasis. Of the 57 patients, 29 (50.9%) were males and 28 (49.1%) were females. The mean age was 60.0 ± 5.33 years. The RAS gene was shown to be mutated in 30 (52.6%) patients and

TABLE 1 Characteristics of metastatic CRC patients.

Characteristic	CRC patients	Controls
Age (years ± SD)	60.0 ± 3.3	65.5 ± 6.83
Sex		
Male	29	14
Female	28	12
RAS gene		
Nonmutated	27	
Mutated	30	
Metastasis		
One organ	17	
More than one organ	40	
Tumor location		
Rectum	14	
Transverse/left colon	34	
Right colon	9	
Metastatic site		
Liver	36	
Lung	8	
Peritoneum	6	
Lymph nodes	5	
Other	2	
Degree of differentiation (primary tumor)		
Well differentiated	6	
Moderately differentiated	31	
Poorly differentiated/undifferentiated	5	

Abbreviation: CRC, colorectal cancer.

40 (70.2%) patients presented with metastasis in more than one organ. Of the control group (n = 26), 14 (53.8%) were males and 12 (46.2%) were females, with a mean age of 65.50 ± 6.83 years. The degree of differentiation could be determined by microscopy in 42 patients at the Pathological Anatomy Service of the Hospital Virgen de las Nieves. Tumor differentiation was expressed as well differentiated, moderately differentiated, and undifferentiated based on the number of glands and the presence of morphological aberrations in them. In general, a tumor well differentiated closely resembles the structure of the tissue where it started. By contrast, a tumor that resembles the original tissue to a lesser extent is termed poorly differentiated, or anaplastic.[28] Finally, all patients received the same type of chemotherapy based on fluoropyrimidine and oxaliplatin.

2.2 | Serum sample collection

Serum samples were collected before receiving any anticancer treatment at the Medical Oncology Service of the Virgen de las Nieves University Hospital (Granada, Spain). All patients were confirmed as metastatic CRC (stage IV). The diagnosis of CRC, which was histologically confirmed by surgery or biopsy and metastatic CRC, was based on imaging studies. In addition, samples from 26 age- and sex-matched healthy controls—from the Andalusian Health System Biobank (Granada, Spain)—were selected so that none of them present any type of tumor or inflammatory pathology. All the subjects recruited as healthy controls completed an in-depth health questionnaire to discard any tumor or inflammatory pathology.

2.3 | Sample preparation for NMR

The preparation of serum samples was carried out following reported methods,[29] with few modifications. Serum samples were immediately stored at −80°C at the time of collection and they were cryopreserved until NMR analysis. Prior to preparation, serum samples were thawed at room

temperature. Subsequently, they were centrifuged for 5 min (at 13,500 rpm), and 180 μL of supernatant was mixed with 400 μL of saline solution (0.9% NaCl in D_2O, containing 3 mM of 3-(trimethylsilyl-)2,2',3,3'-tetradeuteropropionic acid (TSP)), as already established.[26,29] After centrifugation for 10 min (at 11,000 rpm, 4°C), 500 μL of supernatant was transferred to 5-mm NMR tubes.

2.4 | NMR experiments

A total of 83 samples (26 from healthy controls and 57 from CRC patients) were recorded at 293 ± 0.1 K using an NMR spectrometer (Bruker Avance III 600) operating at a proton frequency of 600.13 MHz, equipped with a thermostatted autosampler of 24 positions and a 5-mm QCI quadruple resonance pulse field gradient cryoprobe. The NMR spectra were acquired using the Carr–Purcell–Meiboom–Gill (CPMG) pulse sequence (98 ms of echo time) including water presaturation (Bruker 1D cpmgpr1d) to attenuate broad signals in spectra from macromolecules and/or proteins.[5,30,31] Samples were measured without rotation, using 16 dummy scans and 128 scans. The acquisition parameters were as follows: size of the free induction decay (FID) signal (TD) = 32 K, spectral width (SW) = 22.0 ppm, acquisition time = 1.24 s, relaxation delay (D1) = 3 s, receiver gain (RG) = 203, FID resolution (FIDRES) = 0.81 Hz, and total echo time = 96 ms. Acquisition and processing of spectra were carried out with TOPSPIN software (version 3.6.3). The spectrometer transmitter was locked to D_2O frequency, and the spectra were automatically phased, baseline-corrected, and calibrated to the TSP signal at 0 ppm. To estimate the longitudinal relaxation parameter T_1 of proton resonances and establish the acquisition time plus a recycle delay always greater than five times the highest determined T_1, inversion recovery with continuous wave (CW) presaturation experiments (Bruker sequence 2dt1irpr_cwvd)[32] were performed in several serum samples. In all cases, relaxation T_1 times were in the range of 332–795 ms.

2.5 | NMR metabolite assignments

The metabolite assignments were carried out through the analysis of 2D NMR experiments (homonuclear and heteronuclear experiments) performed in a representative serum sample, together with the use of some NMR databases (Chenomx and public NMR databases such as HMDB) and literature data.[29,33,34] Concerning the 2D NMR experiments necessary for the assignments, $^1H - {}^1H$ total correlation spectroscopy (TOCSY) and $^1H - {}^{13}C$ heteronuclear multiple bonds coherence (HMBC) were recorded using standard Bruker sequences. The acquisition parameters for TOCSY were: D1 = 1.2 s, SW = 7211.54 Hz in F2 and 7201.60 Hz in F1 and RG = 203. The TOCSY spectrum was processed using the sine-bell window function (SSB = 2.0). The HMBC spectrum was acquired using the following parameters: D1 = 1.0 s, SW = 7812.50 Hz in F2 and 37730.04 Hz in F1, with RG = 203.

2.6 | Determination of fatty acids

The analysis of fatty acids profile in serum samples included transesterification and transmethylation processes prior to gas chromatography (Agilent Technologies 6890 N Series Gas Chromatograph, Santa Clara, CA, USA) coupled to flame-ionization detection (GC-FID), as described elsewhere, and therefore we only refer to total fatty acids.[35]

2.7 | Statistical analysis

Each NMR spectrum was divided into 0.04 ppm chemical shift bins from δ_H 0.2 to 10.0 ppm using AMIX 3.9.15 (Bruker BioSpin GmbH, Rheinstetten, Germany), and buckets were obtained by integrating the corresponding spectral areas. The region of δ_H 4.90–4.70 ppm, which contains residual signals of H_2O suppression, was excluded from the bucketing and analysis. Normalization was performed on the data prior to statistical analyses, by dividing the area of each bucketed region by the total area of the evaluated ppm range. MVDA were performed on the data matrix obtained using SIMCA-P software (v. 17.0, Umetrics). Exploratory and unsupervised analysis as principal component analysis (PCA), and supervised models as Orthogonal Projections to Latent Structures Discriminant Analysis (OPLS-DA), were applied, and they were scaled to Pareto. For both models, scores and loadings plots were generated, and for the OPLS-DA model, R^2 and Q^2 cumulative values were given, together with the coefficient of variation-analysis of variance (CV-ANOVA) parameter validation (at the level of significance of $p < 0.05$), to test the accuracy of the model.

    A nonlinear Random Forest (RF) model was also employed for the assessment of further comparisons through the statistical analysis of one factor option from the online tool MetaboAnalyst.[36] This algorithm uses an ensemble of decision trees (forest), where each of them is built on a bootstrap sample of the training portion of the dataset through a random subset of selected variables. After that, the number of trees that identify

a sample with a specific class is interpreted as the probability of fitting in a particular class, quantified with the mean decrease in accuracy (MDA) value. The general error of this model was calculated from the out-of-bag (OOB) estimate.[37]

Univariate area under the receiver operating characteristic curve (AUROC) analyses, along with t-tests ($p < 0.05$), were performed with the purpose of obtaining the main potential biomarkers between patients and healthy controls.

Furthermore, AUROC analyses of the metabolites by employing linear (PLS-DA) and nonlinear Support Vector Machine (SVM) and RF methodologies were applied in order to validate the results, selecting biomarkers with an area under the curve (AUC) value higher than 0.7.[38] These receiver operating characteristic (ROC) curve analyses were generated by Monte Carlo crossvalidation using balanced subsampling. Two-thirds of the samples were employed as a training set, and the corresponding important features from the whole dataset were used to build the classification model. The validation of these potential biomarkers (those with an AUC value > 0.7) was finally accomplished employing the remaining one-third of the samples as a test set. This assessment was accomplished through the online tool MetaboAnalyst, employing the Biomarker Analysis option.

2.8 | Metabolite quantification and calculation of ratios

Quantification of some relevant metabolites was performed in the NMR spectra by the integration of specific signals with respect to the signal of the TSP internal standard (Table S1). It is important to note that for quantification purposes we assume that resonances of interest and TSP had similar T_2 values. Glutamate, glutamine, pyruvate, and alanine contents were quantified in both groups of samples, and the glutamate-to-glutamine (GGR) and pyruvate-to-alanine (PAR) concentration ratios were calculated. Statistical differences between both ratios were validated through Student's t-test ($p < 0.05$).

2.9 | Metabolomics pathway analysis

A pathway analysis of differential metabolites, consisting of enrichment analysis and pathway topological analysis, was performed with the Metabolomics Pathway Analysis (MetPA) attribute within the MetaboAnalyst online tool.[36] For the enrichment of the path, a global test algorithm was employed. The *Homo sapiens* metabolic pathways library was chosen. Pathways were considered significantly enriched if they satisfied the criteria that follows p value less than 0.05, Holm p values (adjusted by the Holm–Bonferroni method) less than 0.05, adjusted p values of the false discovery rate (FDR) less than 0.05, impact of the route more than zero, and number of metabolites hits in the metabolic pathway more than one.

2.10 | Correlation analysis of metabolites with clinical features

In this study, for quantitative variables, two group comparisons were performed using the Student's t-test when the normality assumption was fulfilled, otherwise the Mann–Whitney U test was used. More than two group comparisons were analyzed using a one-way ANOVA or its nonparametric alternative, the Kruskal–Wallis test when the normality assumption was violated. Normality and homoscedasticity assumptions were verified using the Anderson–Darling and Fligner–Killeen tests, respectively. For all the analyses, metabolites with a high linear correlation ($r_{Pearson} > 0.8$) were excluded from the analysis to avoid possible collinearity phenomena when fitting multivariable models. All the analyses were performed with R Software, version 4.0.5.[39]

In the association of the studied metabolites with the survival, a Cox proportional hazard model was fitted taking the 10 metabolites as the response variable. Subsequently, a variable selection step was carried out according to the stepwise methodology to keep the model with the best fit according to the Akaike Information Criterion (AIC). In addition, we verified with a Therneau test that the main hypothesis of proportional hazards was satisfied.

Regression models were adjusted to study the association between KRAS gene status, degree of differentiation of the tumor (anatomopathological study) and location of metastases, and the concentration of metabolites. All these models were adjusted using the 10 selected metabolites as covariates, and the best model was selected with a stepwise procedure according to their AIC. Binomial logistic regression was fitted to study the association between the KRAS gene status and the metabolites. Multinomial logistic regression was considered for the location of metastasis, while the degree of differentiation of the tumor was analyzed at a multivariable level by fitting an ordinal logistic regression model. Goodness-of-fit of binomial logistic regression was assessed with a Hosmer–Lemeshow test. The hypothesis of proportional odds for the ordinal logistic regression model was verified with a Brant test. When a model has significant coefficients, its predictive ability was assessed by using a leave-one-out crossvalidation procedure.
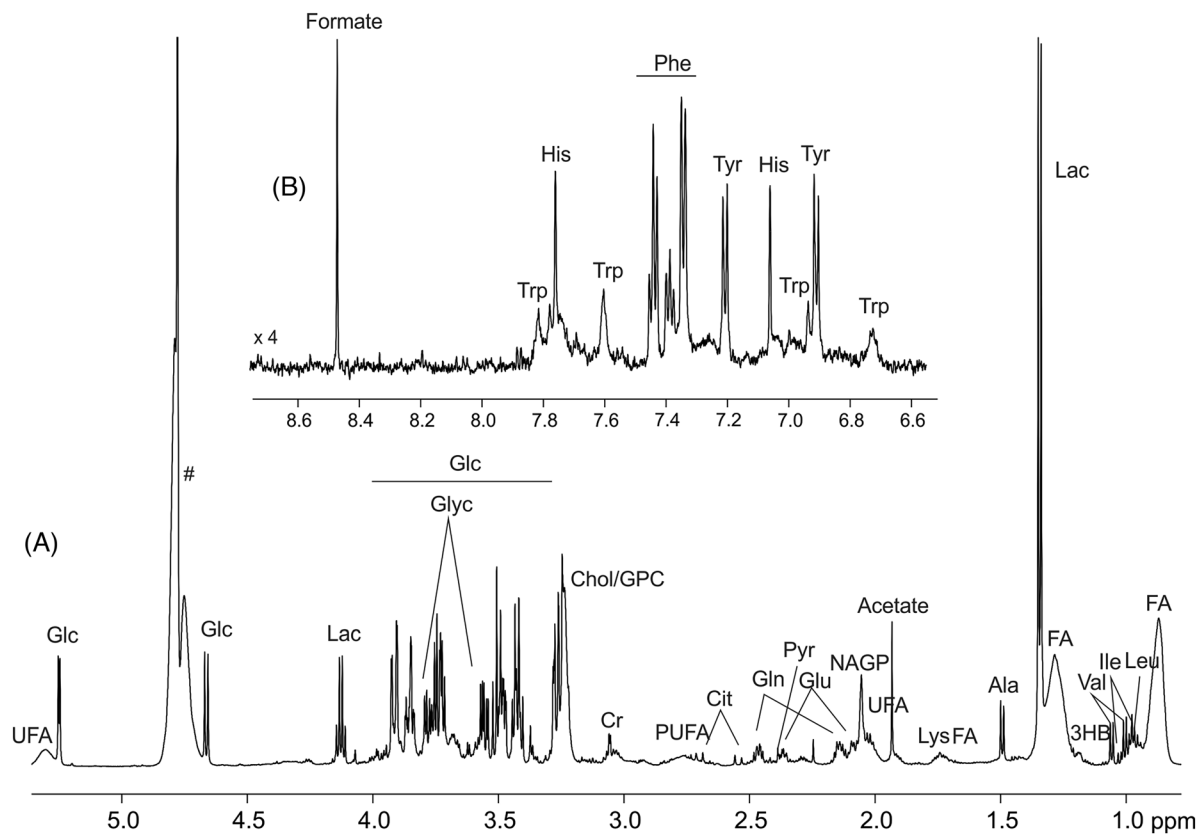
FIGURE 1 (A) Subregion of a representative ^{1}H NMR spectrum (from δ_H 0.8 to 5.3 ppm) obtained at 600 MHz of a serum extract (from the CRC group); (B) Aromatic region of the same spectrum (from δ_H 6.5 to 8.7 ppm). "#" refers to the water suppression signal. 3HB, 3-hydroxybutyrate; Ala, alanine; Chol, choline; Cit, citrate; Cr, creatine; CRC, colorectal cancer; FA, fatty acids; GPC, glycerophosphocholine; Glc, glucose; Gln, glutamine; Glu, glutamate; Glyc, glycerol; His, histidine; Ile, isoleucine; Lac, lactate; Leu, leucine; Lys, lysine; NAGP, N-acetylglycoproteins; Phe, phenylalanine; PUFA, polyunsaturated fatty acids; Pyr, pyruvate; Trp, tryptophan; Tyr, tyrosine; UFA, unsaturated fatty acids; Val, valine.

3 | RESULTS AND DISCUSSION

3.1 | Metabolite profiling of serum samples

A large number of metabolites have been identified, as specified in Figure 1 and Table S1, belonging primarily to classes of amino acids (valine, iso-leucine, leucine, lysine, alanine, glutamate, glutamine, tyrosine, phenylalanine, histidine, and tryptophan), derived organic acids and ketone bodies (3-hydroxybutyrate, acetate, pyruvate, lactate, citrate, and formate), sugars (glucose) and fatty acids (saturated [FA], unsaturated [UFA], and poly-unsaturated fatty acids [PUFA]), among others. Figure S1 shows a comparison between representative spectrums of a serum sample from a healthy control. GC-FID analysis revealed palmitoleic, oleic, and linoleic acids as the main fatty acids present in the assayed serum samples, together with others present in minor concentrations, as given in Table S2.

Regarding the "choline" region at ~ δ_H 3.23 ppm, two partially overlapped singlets were observed that were assigned to choline (Chol) and glycerophosphocholine (GPC) as in previous studies.[40] However, we are aware that other derivatives of choline, such as phosphatidylcholine, lysophosphatidylcholine, or acetylphosphatidylcholine, are possibly formed.[29]

3.2 | Metabolic changes between control and cancer samples

PCA over the total number of cases was applied as a first exploratory analysis to reveal the main trends in ^{1}H NMR data for each group of samples and to detect possible outliers. Figure 2A shows the scores plot obtained from PCA of PC1 versus PC2, explaining 41% and 17% of the total vari-ance, respectively. Even although most samples from the CRC group are placed in the lower part and control samples are mainly located in the upper part of this plot, PCA showed a very slight clustering trend, in which no outliers were excluded. Therefore, a supervised analysis was
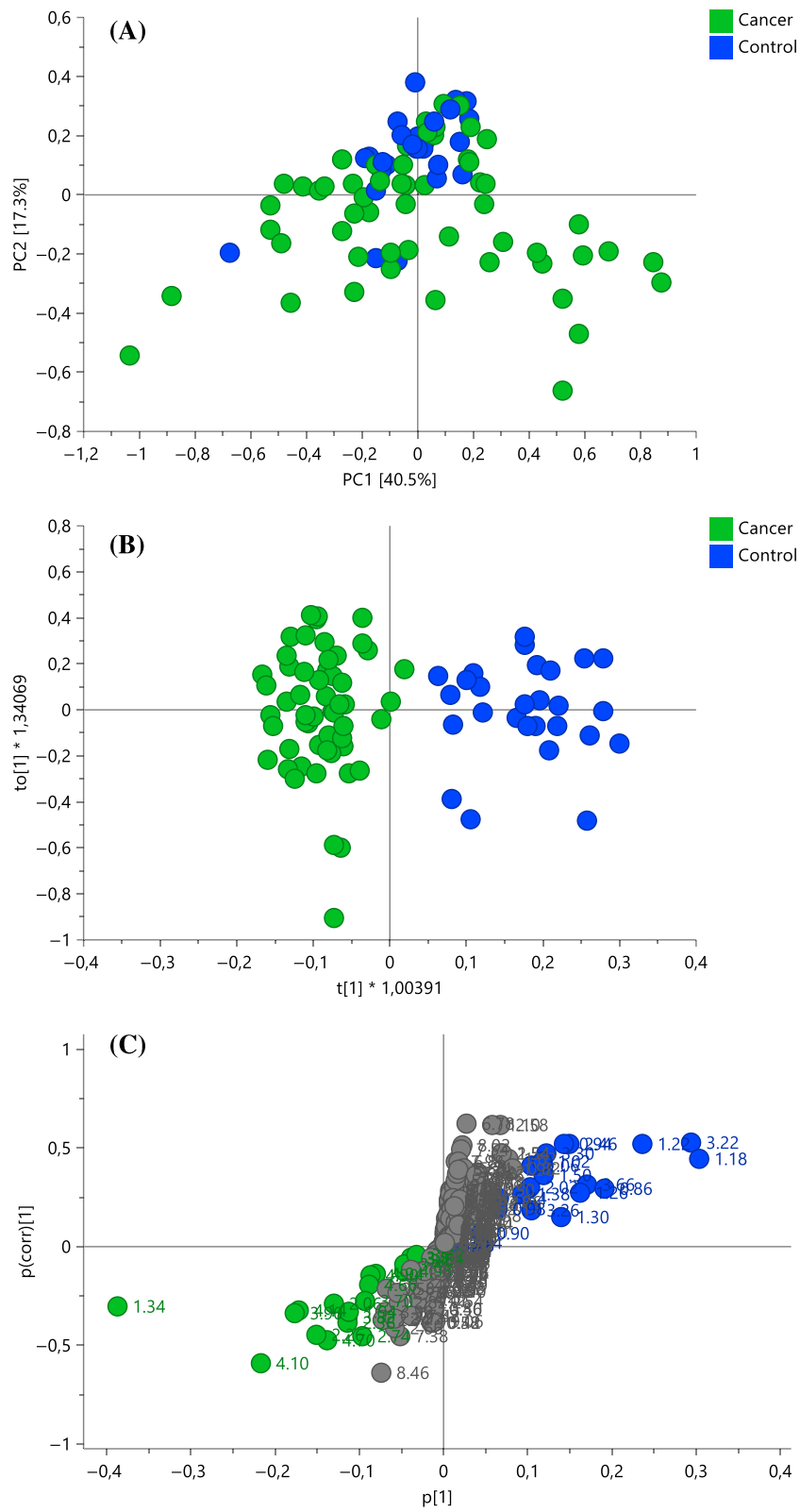
FIGURE 2 Legend on next page.

FIGURE 2 ^{1}H NMR (600 MHz) fingerprint discrimination between CRC (in green) and control (in blue) groups. (A) Scores plot of a PCA model applied to ^{1}H NMR data (scaling was done to Pareto); (B) Scores plot; and (C) S-plot obtained after the application of an OPLS-DA model to the ^{1}H NMR data (scaling was done to Pareto, $R^2X = 0.765$, $R^2Y = 0.857$, Q^2 [cum] = 0.707, CV-ANOVA = 8.236×10^{-22}). The S-plot revealed the main loadings (with VIP > 1) that were responsible for the discrimination of CRC samples—lactate (1.34, 4.10, 4.14 ppm), acetone (2.26 ppm), acetate (1.94 ppm), glutamate (2.06, 2.38 ppm), pyruvate (2.38 ppm), and glucose (3.42, 3.46, 3.50, 3.54, 3.70, 3.82, 3.86, 3.90, 4.66 ppm)—and also for the discrimination of control samples: 3-hydroxybutyrate (1.18, 1.22, 3.66 ppm), choline and glycerophosphocholine (3.22, 3.26 ppm), glutamine (2.46 ppm), leucine (0.94, 0.98 ppm), isoleucine (0.94, 1.02 ppm), valine (1.02, 1.06 ppm), alanine (1.50 ppm), and fatty acids (0.86, 0.90, 1.26, 1.30, 2.02, 5.34 ppm). CRC, colorectal cancer; CV-ANOVA, coefficient of variation-analysis of variance; OPLS-DA, Orthogonal Projections to Latent Structures Discriminant Analysis; PCA, principal component analysis; VIP, variable importance in projection.
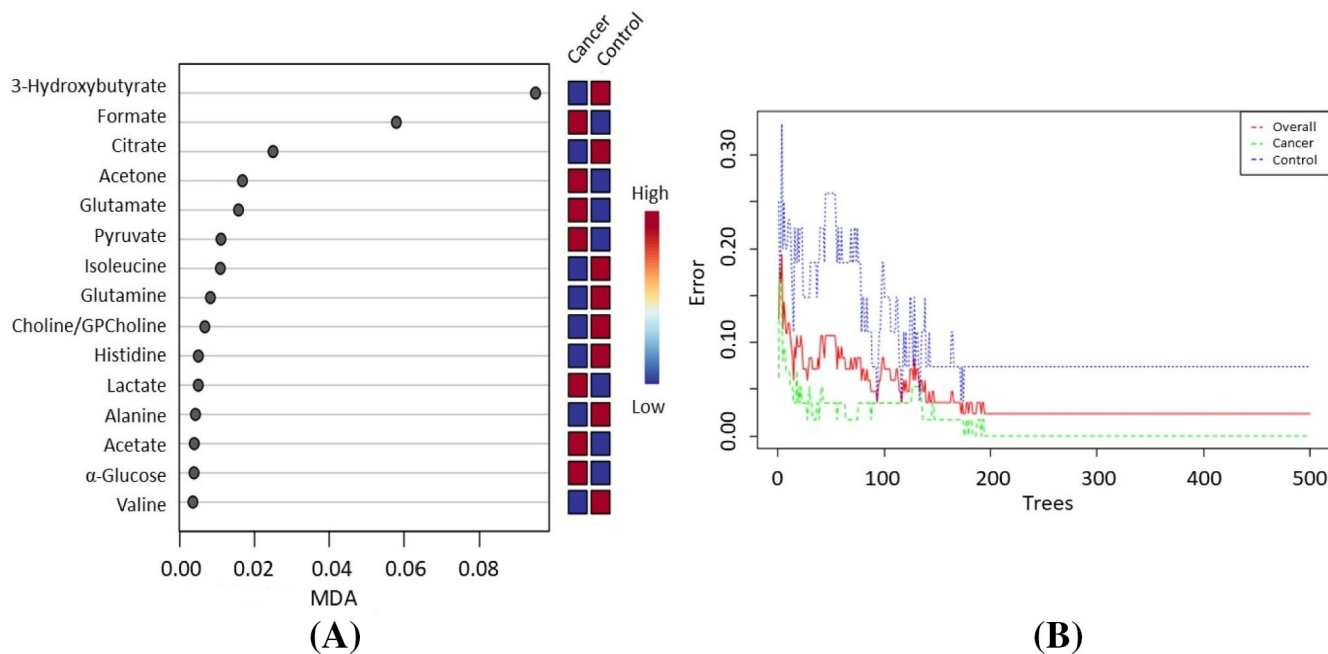

(A) **(B)**

FIGURE 3 (A) Significant features recognized by Random Forest. Those are ranked by the mean decrease in classification accuracy (MDA) when they are permuted for the CRC and control groups. (B) Cumulative error rates by Random Forest classification depending on the number of trees. The red line represents the overall error rate; the green and blue lines indicate the CRC and control error rates, respectively. CRC, colorectal cancer.

performed by applying an OPLS-DA model to the ^{1}H NMR dataset, which correlates the spectral data information with information on sample classes, in this case corresponding to control or cancer labels. The OPLS-DA scores plot of Figure 2B revealed a strong discrimination of the samples between the two groups with good descriptive statistics from model fitting such as goodness-of-fit (R^2) and goodness-of-prediction (Q^2). The subsequent analysis of loadings plot, represented by an S-plot (Figure 2C), revealed the NMR regions containing signals of the metabolites responsible for the discrimination between the CRC and control groups. The loadings with a variable importance in projection (VIP) higher than 1 are colored in green and blue for cancer and control samples, respectively.

CRC samples showed a higher concentration of lactate, acetone, acetate, glutamate, pyruvate, and glucose compared with the healthy control group, which in turn revealed an increase of 3-hydroxybutyrate, choline, GPC, glutamine, leucine, isoleucine, valine, alanine, and fatty acids, mainly UFA, palmitoleic and oleic acids, which were those present in blood serum, as determined by GC-FID.

Additionally, a RF (500 trees and seven predictors) classification was applied to the total number of cases dataset to reflect clustering patterns along the healthy control and CRC groups, due to its robustness for high dimensional data assessments. A list of a total of 15 potentially relevant metabolites was obtained, highlighting the performances of 3-hydroxybutyrate and, in a second level of accuracy, the metabolite formate (Figure 3A). The former metabolite contributes to this model with a mean decrease in classification accuracy (MDA) of 0.082, verifying its value as a potential biomarker of CRC, as can also be appreciated in the OPLS-DA model, while the latter metabolite displays a lower MDA of 0.062, which highlights some latent value as a biomarker. Some other coincidental important metabolites that appeared in both the linear and nonlinear models were lactate, acetone, acetate, glutamate, pyruvate, glucose, glutamine, isoleucine, valine, choline, glycerophoshocholine, and fatty acids, reinforcing their value as relevant feasible biomarkers of CRC. The OOB error value was 0.024 for the classification among cancer and control samples (Figure 3B).
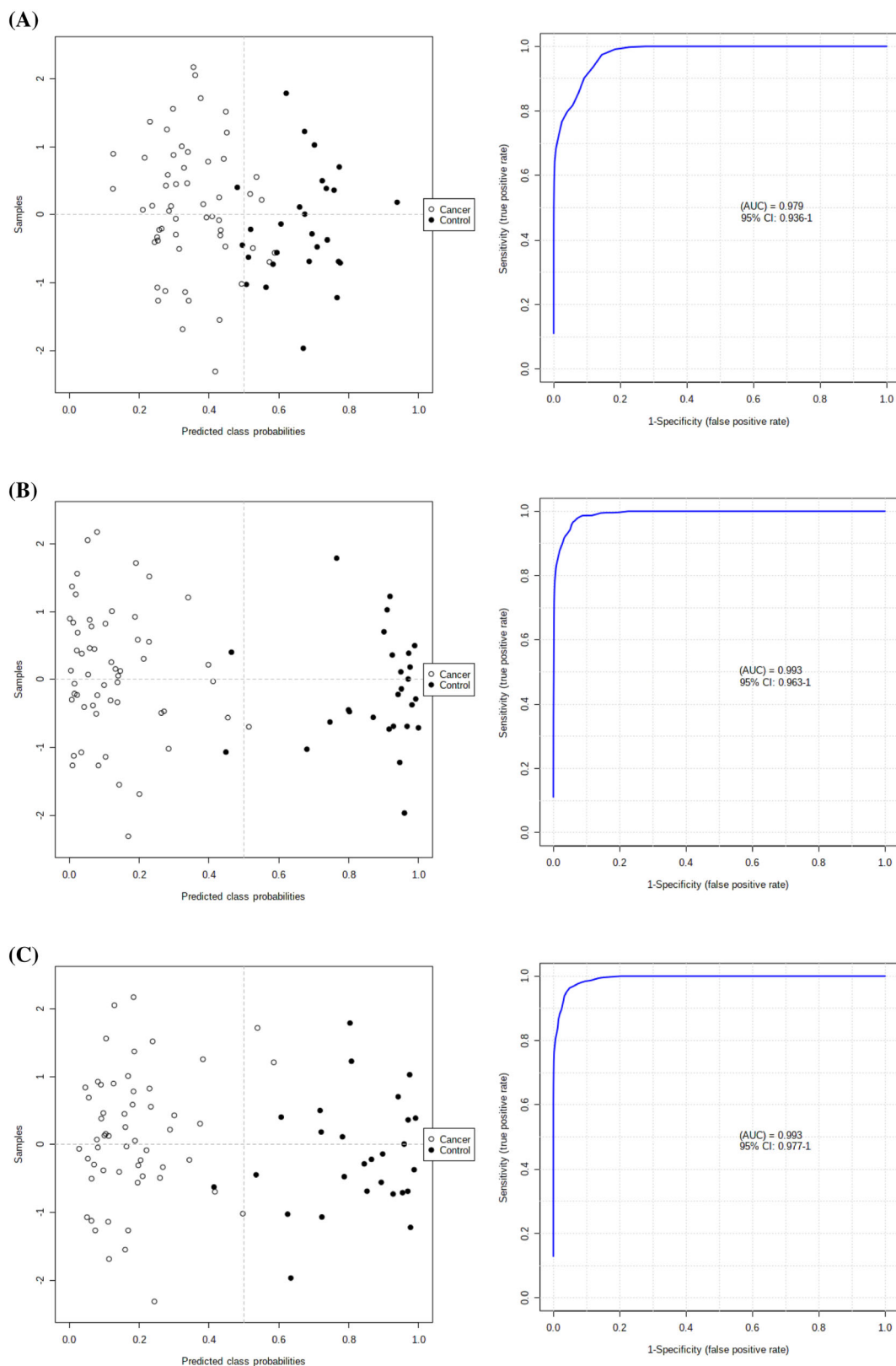
FIGURE 4 Quantitative evaluation of the diagnostic performance for putative biomarkers. AUROC analysis was performed to evaluate the performance of the 12 putative biomarkers employing (A) PLS-DA, (B) SVM, and (C) Random Forest. AUC values of 0.979, 0.993, and 0.993, and average accuracies of 0.906, 0.947, and 0.956, were obtained for each model, respectively. AUC, area under the curve; AUROC, area under the receiver operating characteristic curve; PLS-DA, Projections to Latent Structures Discriminant Analysis; SVM, Support Vector Machine.

These upregulated and downregulated metabolites found in our study are consistent with those found in previous studies,[5,41–43] and those already reviewed.[26] In fact, the "Warburg effect", which describes an increase in the glycolysis process in cancer cells, gives strong support to our results. For instance, an increase in glucose, involved in the first step of glycolysis, and in pyruvate and lactate, the intermediate and the endpoint of this metabolic pathway,[44] respectively, were observed in the serum samples of CRC patients. Gu et al.[5] determined that the content in lipids was higher for healthy controls and patients with colorectal disease other than cancer (colorectal adenomatous polyps) than for CRC patients, similar to our findings in this study, and may suggest that cancer cells intensify fatty acid β-oxidation to support the energy demand of cancer cell proliferation.

Additionally, classical univariate AUROC analyses were performed for each of the obtained potential biomarkers, together with its corresponding t-test and fold-change values. As a result, 12 metabolites were shown to be more significantly different between the CRC and control groups, with an AUC of at least 0.70 (Table S3). This value highlights an increased biomarker ability in the clinical setting.

Four of these metabolites revealed an AUC higher than 0.8, corresponding to 3-hydroxybutyrate, glutamine, choline, and GPC, and therefore were assigned as those with the highest potential as serum biomarkers for CRC patients.

The performances of the 12 potential biomarkers were validated through multivariate AUROC analysis of PLS-DA, SVM, and RF models, as can be appreciated in Figure 3. These metabolites had the ability to discriminate metastatic CRC patients and healthy controls with AUC values of 0.978, 0.993, and 0.993, with average accuracies of 0.906, 0.947, and 0.956 for the PLS-DA, SVM, and RF models, respectively (Figure 4).
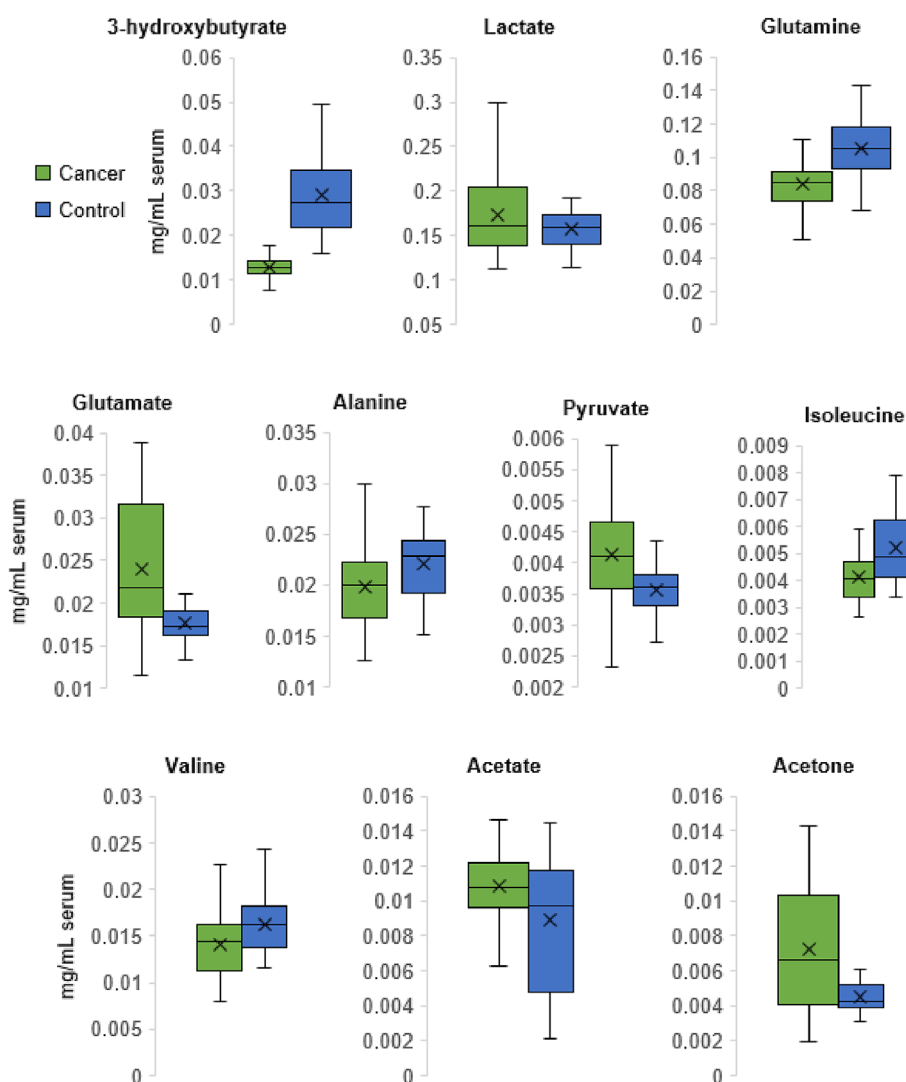

FIGURE 5 Quantification of biomarkers (in mg of metabolite/mL serum) with an AUC higher than 0.7. Green and blue boxes represent colorectal cancer patients and controls, respectively. In each boxplot, the crosses represent the mean value, and the horizontal lines represent the median value. Choline and GPC were considered together because of the overlapping of their signals, so for that reason its boxplots do not appear in this figure. Concentration differences were all statistically significant ($p < 0.05$). AUC, area under the curve; GPC, glycerophosphocholine.

Although these results suggest good discrimination accuracy, future validation studies in a new set of patients will be necessary to precisely determine the diagnostic value of this candidate biomarker panel.

Boxplots for the whole set of biomarkers are given in Figure 5, in which it is interesting to observe how 3-hydroxybutyrate, glutamine, alanine, isoleucine, and valine are downregulated in CRC patients, whereas lactate, glutamate, pyruvate, acetate, and acetone are at higher concentrations in these patients. Choline and GPC levels are also reduced in individuals with CRC; however, their boxplots do not appear in the figure because their signals overlap each other due to broadness imposed by fast T2-relaxation, especially in GPC, making it difficult to accurately measure them separately. Supporting our results, decreased glutamine, alanine, and valine levels have been previously reported in CRC patients compared with either healthy controls or patients with nonmalignant colorectal disease.[5] Also, in line with our results, these authors observed higher glutamate concentrations in CRC patients than in the other two study groups. On the contrary, 3-hydroxybutyrate and isoleucine were found to be downregulated in our CRC data, but were observed as upregulated in CRC patients by these authors. These discrepancies could be because the authors included different CRC stages, whereas in our study, all of the patients were in the metastatic phase.

3.3 | Pathway analysis

Because advanced medical treatments target specific pathways, knowledge about activated or silenced pathways is key for the future development of personalized cancer treatments. Metabolite-based biomarkers are always involved in specific pathways and are used as effective probes to monitor if the routes in which they are present are tackled. It is important to ascertain the hierarchy of metabolic pathways altered in CRC, because this would enable understanding the impact of the disease and how best to plan the treatment. For this reason, a MetPA was performed
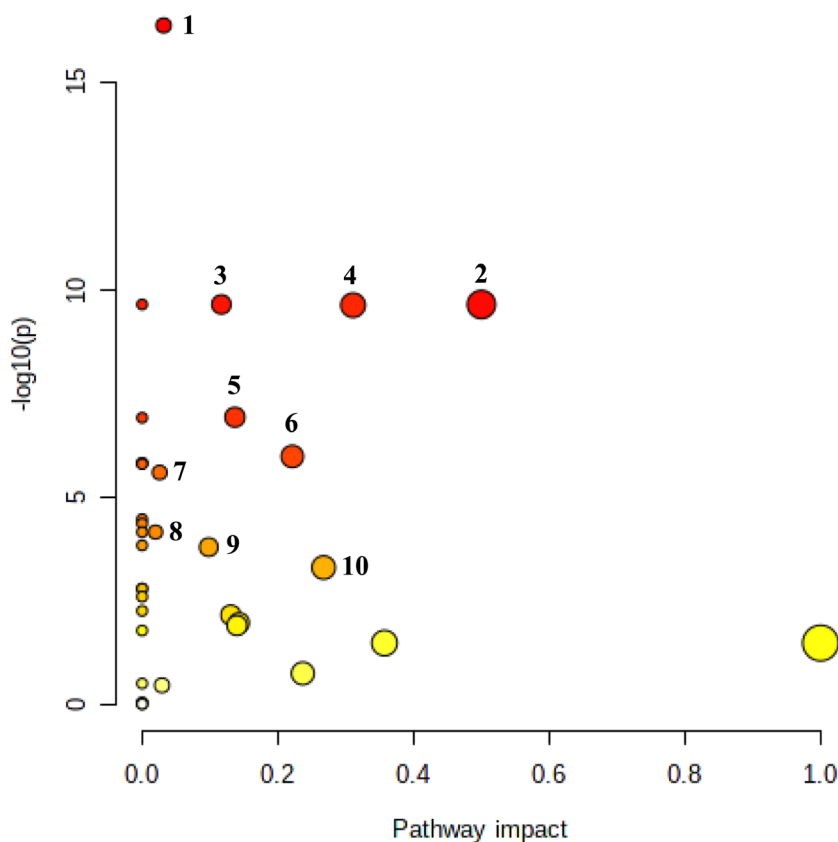

FIGURE 6 Metabolic pathway analysis of the altered metabolic routes in colorectal cancer. A color gradient from yellow (less significant) to red (most significant) allows to define the more affected metabolic routes. Pathways that satisfy the criteria (impact index for each metabolic route > 0, Holm and FDR-adjusted $p < 0.05$ and number of matching metabolites in the pathway > 1) were considered significantly enriched: 1 - Glyoxylate and dicarboxylate metabolism, 2 - D-glutamine and D-glutamate metabolism, 3 - Arginine biosynthesis, 4 - Alanine, aspartate, and glutamate metabolism, 5 - Citrate cycle (tricarboxylic acid [TCA] cycle), 6 - Histidine metabolism, 7 - Glycerophospholipid metabolism, 8 - Glutathione metabolism, 9 - Arginine and proline metabolism, and 10 – Pyruvate metabolism. Values of concentration quantification of the metabolites were used for the analysis. Significantly altered metabolic routes and more information concerning statistical analysis can be found in Table S4. FDR, false discovery rate.

with the help of the software MetaboAnalyst.[36] The relevant metabolic pathways, along with the number of matching metabolites, impact on metabolic pathway, p value, Holm p value, and impact index for each metabolic route, can be found in Table S4. Figure 6 illustrates the pathway analysis of quantitative metabolomic data, where the most significant altered pathways are given in red.

The metabolic pathways that are affected by CRC with higher impact index are "D-glutamine and D-glutamate metabolism", "pyruvate metabolism", and "alanine, aspartate and glutamate metabolism". "Pyruvate metabolism" involves three metabolites that were classified as potential CRC biomarkers in our study: pyruvate, lactate, and acetate. As mentioned previously, this is in accordance with the Warburg effect, which establishes that cancer cells have an altered metabolism to survive, so they significantly increase glucose uptake and fermentation of glucose to lactate, even in the presence of enough oxygen and with fully functioning mitochondria.[45,46] Therefore, the observed higher glycolytic rate helps anabolism in proliferating tissues, such as primary tumors or metastasis. It can also be employed as a fuel source by cancer cells after conversion back to pyruvate, where oxygen levels are sufficient to produce ATP. Pyruvate is presented as the final product of glycolysis (which is the major generator of this metabolite), but it can also be generated by other sources, as lactate oxidation or alanine transamination. The alteration of this metabolism in cancer cells can constitute an effective target to modulate for the development of drugs to fight against cancer.[47]

"Alanine, aspartate and glutamate metabolism", which is also involved in CRC, includes alanine, citrate, glutamine, glutamate, and pyruvate as metabolite hits. As already mentioned, alanine and glutamine decreased in CRC samples, whereas glutamate and pyruvate increased their contents in this group. This makes sense, because alanine is taken up by cancer cells and deaminated to pyruvate as a significant carbon source.[48] The study conducted by Sirniö et al.[43] also reported lower levels of amino acids in CRC serum, such as alanine, valine, leucine, and isoleucine, which was mainly associated with advanced cancer stages. Another important fact is that glutamine is not processed in the same way in cancer cells as in normal cells, so they overexpress an enzyme, glutaminase, which converts glutamine to glutamate.[49] These cells also use glutamine to generate energy, and sometimes it is also converted to pyruvate,[50] which is in accordance with the decrease in glutamine and the increase in pyruvate and glutamate concentrations. Consequently, Budczies et al.[49] already used the ratio of glutamate to glutamine (GGR) as a predictor of cancer and found that tumoral cells have higher GGR than normal cells, which could be potential evidence of cancer. Cluntun et al.[51] have also proposed that targeting glutamine metabolism could also be used as a potential anticancer therapy. All the connected metabolic routes affected by CRC in this work, along with GGR and pyruvate-to-alanine ratio (PAR) (described below) boxplots, are given in Figure 7 for both control and CRC patients.

As expected, the mean GGR value obtained for cancer samples (0.28 ± 0.09) was significantly higher ($p < 0.05$) than for control samples (0.17 ± 0.02). However, we must be cautious, because GGR is already described as a characteristic ratio for some diseases, as coronary artery disease, schizophrenia, and even in COVID-19.[52–54]

For this reason, and attending to the unraveled upregulated and downregulated metabolites, we have also established a new potential biomarker based on the PAR, obtaining a significantly higher ($p < 0.05$) ratio in CRC patients (0.24 ± 0.06) than in healthy controls (0.16 ± 0.02). Thus, we performed classical univariate AUROC analyses for both ratios, achieving the same AUC value of 0.94 in both cases. These correspond to high rates that position these factors as feasible great biomarkers. Thus, GGR and PAR, taken together, are therefore proposed as potential indicators of the presence of metastatic CRC, although it is always recommended to use the complete pattern of proposed biomarkers for a comprehensive analysis. To the best of our knowledge, the PAR biomarker has never been employed in CRC diagnosis, although it could be viewed as an indicator of how transaminases activity effectively transforms pyruvate into alanine in the cytosol.[48]

Other metabolites that have been found to be significant in the discrimination between the control and CRC serum samples are 3-hydroxybutyrate and fatty acids. 3-hydroxybutyrate is a denominated "ketone body" and is the main representative of this group in animal cells. Dmitrieva-Posocco et al. have recently shown the CRC suppressor role of 3-hydroxybutyrate, both in murine models and human CRC samples.[55] One of its functions is to provide acetoacetyl- and acetyl-COA for the synthesis of cholesterol, fatty acids, and other lipids.[56] Therefore, if 3-hydroxybutyrate is downregulated in CRC patients, fatty acids are also downregulated, as occurs in our spectra. In agreement with our findings, it has been previously reported that fatty acids, and more specifically PUFA, decreased its content in CRC patients.[57] Interestingly, CRC tissue has shown higher PUFA levels than normal tissue; however, serum samples derived from CRC patients presented lower PUFA concentrations than those derived from healthy controls.[42]

3.4 | Correlation analysis of metabolites with clinical features

Finally, we searched for a possible relation of these metabolites with the most relevant clinical features of the patients, which included (i) overall survival from diagnosis, (ii) progression-free survival, (iii) KRAS gene status, (iv) degree of differentiation of the tumor, and (v) location of metastases. Previously, a correlation analysis was performed to exclude high correlated metabolites ($r_{Pearson} > 0.8$) to avoid possible collinearity phenomena when fitting multivariable models. From this study, beta-glucose, lactate, and leucine were removed because they were shown to be highly correlated.

For the overall survival from diagnosis, our Cox model showed on one hand that 3-hydroxybutyrate (HR = 1.781 [1.099, 2.887]) and glutamate (HR = 1.899 [1.106, 3.260]) acted as risk factors, while acetate (HR = 0.057 [0.007, 0.498]) was a protective factor. Interestingly and according to this result, Tran et al.[58] have recently proposed the maintenance of a particular acetate concentration as a complementary strategy
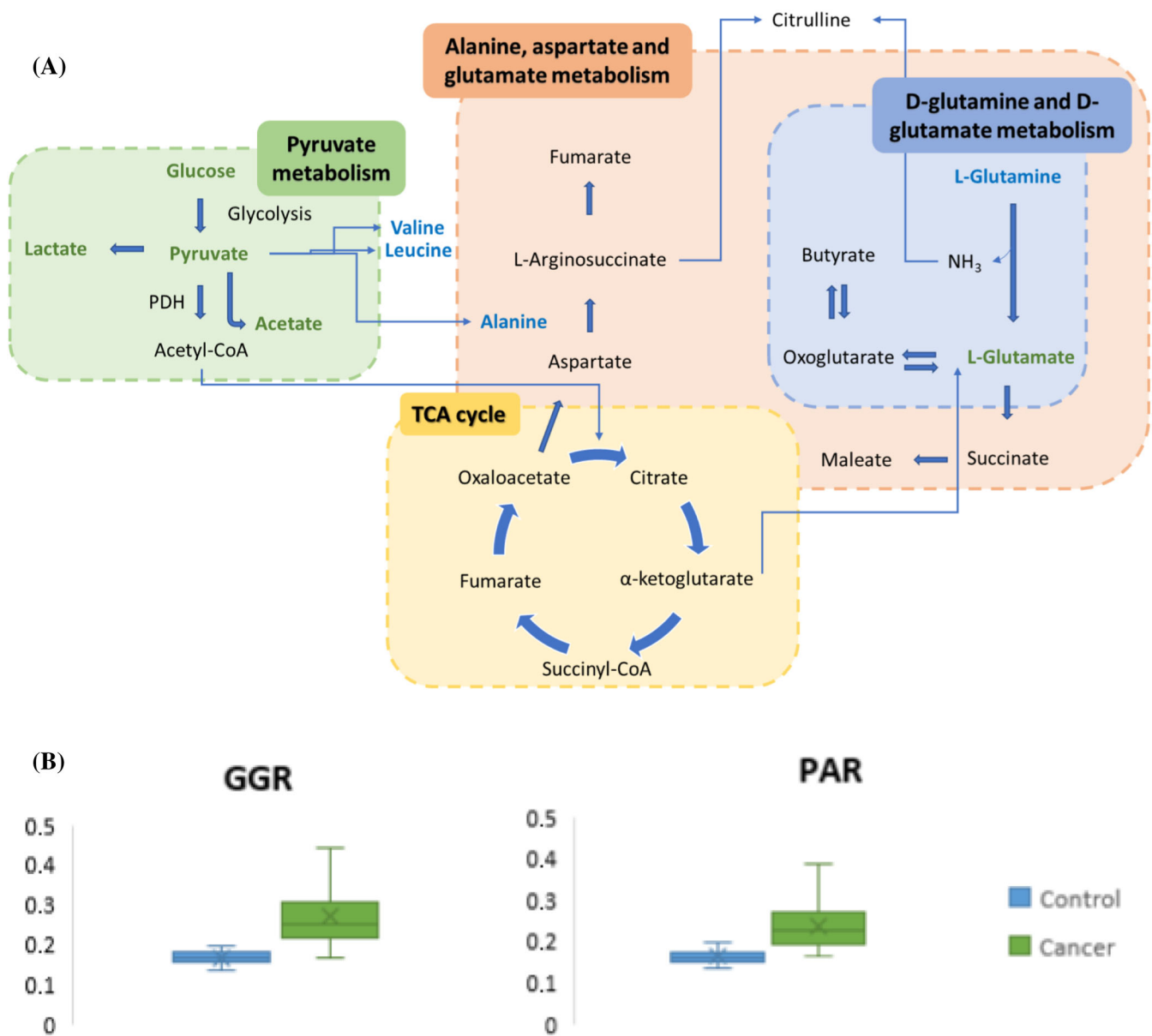
FIGURE 7 (A) Metabolic pathways affected by colorectal cancer; those metabolites in green and blue are biomarkers that increase and decrease, respectively, in the serum of CRC patients; (B) Boxplots for the calculated glutamate-to-glutamine (GGR) and pyruvate-to-alanine (PAR) ratios ($p < 0.05$). CRC, colorectal cancer.

for cancer treatment because the acetate-mediated decreased PVR/CD155 expression in cancer cells can potentiate the antitumor immunity in the tumor microenvironment. Moreover, the results of 3-hydroxybutyrate could be related to its importance in the tumor metabolic ecology, where 3-hydroxybutyrate levels, together with other metabolites, have been proposed as a key factor to examine the efficacy of drugs targeting tumor metabolism.[59]

On the other hand, glutamate was the only metabolite related to the progression-free survival of our patients (HR = 1.904 [1.149, 3.156]). This nonessential amino acid is a major bioenergetic substrate and its high levels are necessary for the proliferation of normal and neoplastic cells,[29] which could explain its possible role in both the overall survival and the progression-free survival of patients. α-Glucose was selected by the stepwise algorithm, too, although its coefficient was not significant. In this case, although proportional hazards are met according to the Therneau test, the model does not improve significantly from a null model ($p_{LR} > 0.05$).

Regarding the degree of tumor differentiation, glutamine (OR = 1.506 [1.001, 2.265], $p = 0.049$) (Figure 8) was associated and shown to act as a risk factor. These metabolites are strongly interconnected and the deamination of glutamine to glutamate, mediated by glutaminase (GLS1), is an essential step in glutaminolysis. It is well demonstrated that glutamine is a substrate to replenish TCA cycle intermediates that are highly consumed in CRC.[31] Interestingly, a study by Song et al.[60] demonstrated that the expression of GLS1 was significantly elevated in CRC in comparison
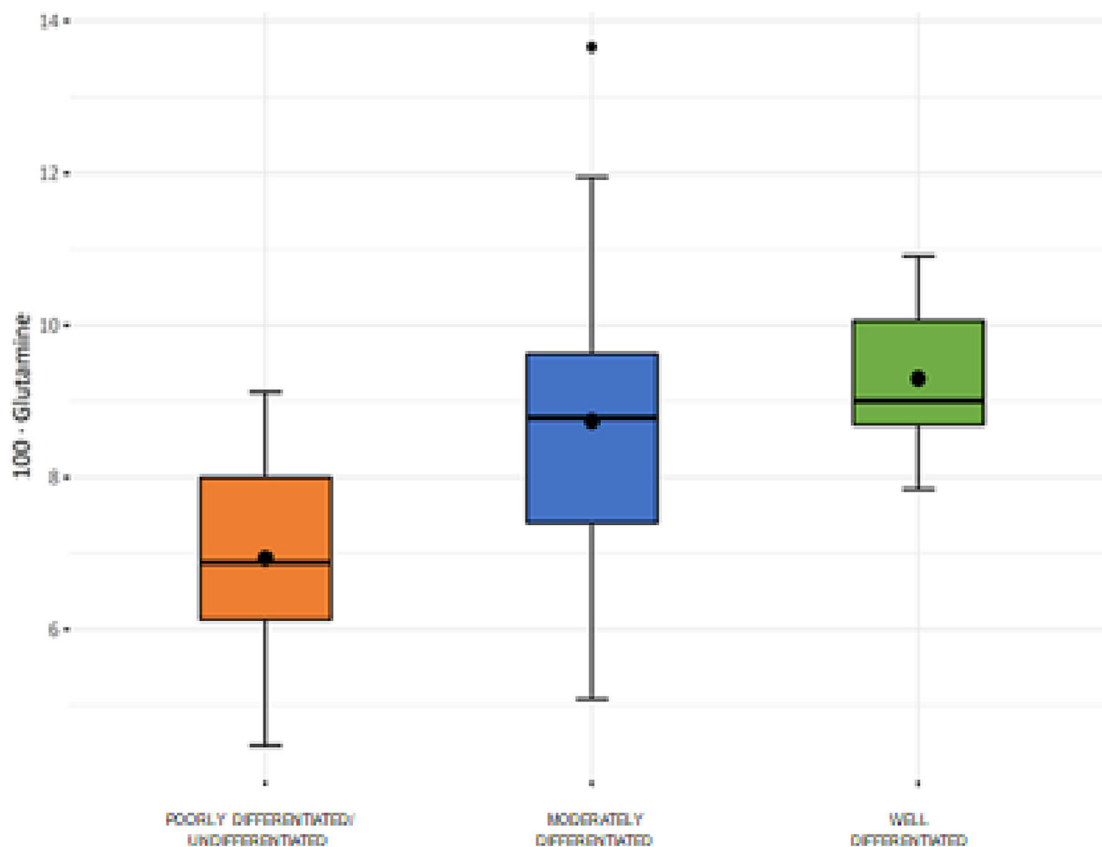
FIGURE 8 Glutamine content (in mg/mL serum) as a function of the degree of tumor differentiation (poorly differentiated/undifferentiated = orange, left; moderately differentiated = blue, middle; well differentiated = green, right). The raw concentration value for each metabolite was multiplied by 100 to improve the interpretation of the coefficients in each model.

with adjacent normal tissues ($p < 0.001$), a fact that is also associated with cell differentiation status and tumor node metastasis stage.[52] On the contrary, when glutamate was selected by the stepwise methodology by including it as a covariate, it improved the model fit but its coefficient was not statistically significant.

The leave-one-out crossvalidation method was performed to check the predictive ability based on the glutamine content. This evaluation shows that our statistical analysis has limited ability to assess the degree of tumor differentiation, with an accuracy of only 69%, which is possibly attributable to an unbalanced sample.

Finally, neither for KRAS gene status, nor for the location of the metastases, was any metabolite that differs significantly between the groups observed at univariate or multivariate levels.

4 | CONCLUSIONS

This study found that the metabolic profile of serum can distinguish between healthy controls and patients with metastatic CRC by using NMR metabolomics in combination with linear and nonlinear multivariate analysis techniques. Some metabolites, such as lactate, acetone, acetate, glutamate, and pyruvate, were found to be present in higher concentrations in the serum of CRC patients, while others, including 3-hydroxybutyrate, choline, GPC, certain amino acids, and fatty acids, were found to be decreased. The performance of these metabolites was confirmed using ROC analysis of different multivariate linear (PLS-DA) and nonlinear (SVM, RF) techniques. The results suggest that CRC causes specific metabolic changes and that these metabolite concentrations could be used as potential diagnostic biomarkers for the disease. Additionally, the study proposed the use of the concentration ratios of GGR and PAR as potential biomarkers for detecting metastatic CRC, as these ratios were found to be significantly higher in CRC samples than in healthy controls. Furthermore, to the best of our knowledge, PAR has not been previously reported in other cancer studies. However, further validation is necessary to confirm these findings, and more research is needed to explore the relationship between metabolic changes and the progression of CRC. In terms of clinical characteristics, it is important to note that acetate is a protective factor for overall survival from diagnosis, while 3-hydroxybutyrate and glutamate are risk factors. Glutamine was also found to be significantly

correlated with the degree of tumor differentiation. These observations suggest a potential method for detecting metastatic CRC. Further studies focusing on metabolic changes at different stages of localized CRC or the presence of metastases in different sites (not mainly in the liver, which is a limitation of our study) are crucial for improving the chances of early diagnosis and treatment.

CONFLICT OF INTEREST STATEMENT

The authors declare no conflicts of interest.

ETHICS STATEMENT

The study was approved by the Ethics Committee of Junta de Andalucía (protocol code PI19/01478; No. 2020522131049; 29 June 2020), conducted in accordance with the Declaration of Helsinki, and written informed consent was obtained from all participants.

ORCID

Ignacio Fernández https://orcid.org/0000-0001-8355-580X

REFERENCES

1. Mattiuzzi C, Lippi G. Current cancer epidemiology. *J Epidemiol Glob Health.* 2019;9:217-222.
2. World Health Organization. *Cancer Today [Internet]*. WHO. 1984. Available from: https://gco.iarc.fr/today/home. Accessed April 24, 2021
3. Sawicki T, Ruszkowska M, Danielewicz A, et al. A review of colorectal cancer in terms of epidemiology, risk factors, development, symptoms and diagnosis. *Cancer.* 2021;13(9):2025.
4. Araghi M, Soerjomataram I, Jenkins M, et al. Global trends in colorectal cancer mortality: projections to the year 2035. *Int J Cancer.* 2019;144:2992-3000.
5. Gu J, Xiao Y, Shu D, et al. Metabolomics analysis in serum from patients with colorectal polyp and colorectal cancer by ^{1}H-NMR spectrometry. *Dis Markers.* 2019;3491852.
6. Tan B, Qiu Y, Zou X, et al. Metabonomics identifies serum metabolite markers of colorectal cancer. *J Proteome Res.* 2013;12(6):3000-3009.
7. Bray F, Ferlay J, Soerjomataram I, et al. Global cancer statistics 2018: GLOBOCAN estimates of incidence and mortality worldwide for 36 cancers in 185 countries. *CA Cancer J Clin.* 2018;68:394-424.
8. Guren MG. The global challenge of colorectal cancer. *Lancet Gastroenterol Hepatol.* 2019;4:894-895.
9. Morano F, Sclafani F. Duration of first-line treatment for metastatic colorectal cancer: Translating the available evidence into general recommendations for routine practice. *Crit Rev Oncol Hematol.* 2018;131:53-65.
10. Illiano P, Brambilla R, Parolini C. The mutual interplay of gut microbiota, diet and human disease. *FEBS J.* 2020;287:833-855.
11. Das V, Kalita J, Pal M. Predictive and prognostic biomarkers in colorectal cancer: A systematic review of recent advances and challenges. *Biomed Pharmacother.* 2017;87:8-19.
12. Cheung AH, Chow C, To KF. Latest development of liquid biopsy. *J Thorac Dis.* 2018;10:S1645-S1651.
13. Maierthaler M, Benner A, Hoffmeister M, et al. Plasma miR-122 and miR-200 family are prognostic markers in colorectal cancer. *Int J Cancer.* 2017;140:176-187.
14. Barault L, Amatu A, Siravegna G, et al. Discovery of methylated circulating DNA biomarkers for comprehensive non-invasive monitoring of treatment response in metastatic colorectal cancer. *Gut.* 2018;67:1995-2005.
15. Tsukamoto M, Iinuma H, Yagi T, et al. Circulating exosomal microRNA-21 as a biomarker in each tumor stage of colorectal cancer. *Oncology.* 2017;92:360-370.
16. Galamb O, Barták BK, Kalmár A, et al. Diagnostic and prognostic potential of tissue and circulating long non-coding RNAs in colorectal tumors. *World J Gastroenterol.* 2019;25:5026-5048.
17. Martín-Blázquez A, Díaz C, González-Flores E, et al. Untargeted LC-HRMS-based metabolomics to identify novel biomarkers of metastatic colorectal cancer. *Sci Rep.* 2019;9(1):20198.
18. Zamani Z, Arjmand M, Vahabi F, et al. A metabolic study on colon cancer using ^{1}H nuclear magnetic resonance spectroscopy. *Biochem Res Int.* 2014;2014:1-7.
19. Hu R, Li T, Yang Y, et al. NMR-based metabolomics in cancer research. *Cancer Metabolomics: Methods and Applications*. Springer International Publishing; 2021:201-218.
20. Jiménez B, Mirnezami R, Kinross J, et al. 1H HR-MAS NMR spectroscopy of tumor-induced local metabolic "field-effects" enables colorectal cancer staging and prognostication. *J Proteome Res.* 2013;12(2):959-968.
21. Monleón D, Morales JM, Barrasa A, et al. Metabolite profiling of fecal water extracts from human colorectal cancer. *NMR Biomed.* 2009;22(3):342-348.
22. Vahabi F, Sadeghi S, Arjmand M, et al. Staging of colorectal cancer using serum metabolomics with ^{1}H NMR spectroscopy. *Iran J Basic Med Sci.* 2017;20(7):835-840.

23. Ritchie SA, Ahiahonu PW, Jayasinghe D, et al. Reduced levels of hydroxylated, polyunsaturated ultra long-chain fatty acids in the serum of colorectal cancer patients: implications for early screening and detection. *BMC Med.* 2010;8:13.

24. Schmidt DR, Patel R, Kirsch DG, et al. Metabolomics in cancer research and emerging applications in clinical oncology. *CA Cancer J Clin.* 2021;71(4):333-358.

25. Spratlin JL, Serkova NJ, Eckhardt SG. Clinical applications of metabolomics in oncology: a review. *Clin Cancer Res.* 2009;15(2):431-440.

26. Salmerón AM, Tristán AI, Abreu AC, Fernández I. Serum colorectal cancer biomarkers unraveled by NMR metabolomics: past, present, and future. *Anal Chem.* 2022;9(1):417-430.

27. Emwas AH, Salek R, Griffin J, Merzaban J. NMR-based metabolomics in human disease diagnosis: applications, limitations, and recommendations. *Metabolomics.* 2013;9:1048-1072.

28. Halvorsen TB, Seim E. Degree of differentiation in colorectal adenocarcinomas: a multivariate analysis of the influence on survival. *J Clin Pathol.* 1988;41(5):532-537.

29. Wojtowicz W, Zabek A, Deja S, et al. Serum and urine ^{1}H NMR-based metabolomics in the diagnosis of selected thyroid diseases. *Sci Rep.* 2017;7(1):9108.

30. Moldovan OL, Rusu A, Tanase C, Vari CE. Glutamate - a multifaceted molecule: endogenous neurotransmitter, controversial food additive, design compound for anti-cancer drugs. A critical appraisal. *Food Chem Toxicol.* 2021;153:112290..

31. Fages A, Duarte-Salles T, Stepien M, et al. Metabolomic profiles of hepatocellular carcinoma in a European prospective cohort. *BMC Med.* 2015;13(1):242.

32. Poggetto DG, Castañar L, Adams RW, Morris GA, Nilsson M. Relaxation-encoded NMR experiments for mixture analysis: REST and beer. *Chem Commun.* 2017;53:7461-7464.

33. Zhao Y, Zhao X, Chen V, et al. Colorectal cancers utilize glutamine as an anaplerotic substrate of the TCA cycle in vivo. *Sci Rep.* 2019;9(1):19180.

34. Luke TDW, Pryce JE, Elkins AC, et al. Use of large and diverse datasets for ^{1}H NMR serum metabolic profiling of early lactation dairy cows. *Metabolites.* 2020;10(5):180.

35. Rodriguez-Ruiz J, Belarbi EH, Sanchez JLG, Alonso DL. Rapid simultaneous lipid extraction and transesterification for fatty acid analyses. *Biotechnol Tech.* 1998;12(9):689-691.

36. Chong J, Wishart DS, Xia J. Using MetaboAnalyst 4.0 for comprehensive and integrative metabolomics data analysis. *Curr Protoc Bioinformatics.* 2019;68(1):e86.

37. Meoni G, Ghini V, Maggi L, et al. Metabolomic/lipidomic profiling of COVID-19 and individual response to tocilizumab. *PLoS Pathog.* 2021;17(2):e1009243.

38. Xia J, Broadhurst DI, Wilson M, Wishart DS. Translational biomarker discovery in clinical metabolomics: an introductory tutorial. *Metabolomics.* 2013;9(2):280-299.

39. R Core Team (Computer Software). R: A language and environment for statistical computing. R Foundation for Statistical Computing. Available from: https://www.R-project.org/. 2021.

40. Embade N, Mariño Z, Diercks T, et al. Metabolic characterization of advanced liver fibrosis in HCV patients as studied by serum 1H-NMR spectroscopy. *PLoS ONE.* 2016;11(5):e0155094.

41. Deng L, Gu H, Zhu J, et al. Combining NMR and LC/MS using backward variable elimination: metabolomics analysis of colorectal cancer, polyps, and healthy controls. *Anal Chem.* 2016;88(16):7975-7983.

42. Mika A, Kobiela J, Pakiet A, et al. Preferential uptake of polyunsaturated fatty acids by colorectal cancer cells. *Sci Rep.* 2020;10(1):1954.

43. Sirniö P, Väyrynen JP, Klintrup K, et al. Alterations in serum amino-acid profile in the progression of colorectal cancer: associations with systemic inflammation, tumour stage and patient survival. *Br J Cancer.* 2019;120(2):238-246.

44. Qiu Y, Cai G, Su M, et al. Serum metabolite profiling of human colorectal cancer using GC-TOFMS and UPLC-QTOFMS. *J Proteome Res.* 2009;8(10):4844-4850.

45. Liberti MV, Locasale JW. The Warburg effect: How does it benefit cancer cells? *Trends Biochem Sci.* 2016;41(3):211-218.

46. Vander Heiden MG, Cantley LC, Thompson CB. Understanding the Warburg effect: the metabolic requirements of cell proliferation. *Science.* 2009;324(5930):1029-1033.

47. Gray LR, Tompkins SC, Taylor EB. Regulation of pyruvate metabolism and human disease. *Cell Mol Life Sci.* 2014;71(14):2577-2604.

48. Vettore L, Westbrook RL, Tennant DA. New aspects of amino acid metabolism in cancer. *Br J Cancer.* 2020;122(2):150-156.

49. Budczies J, Pfitzner BM, Györffy B, et al. Glutamate enrichment as new diagnostic opportunity in breast cancer. *Int J Cancer.* 2015;136(7):1619-1628.

50. Altman BJ, Stine ZE, Dang CV. From Krebs to clinic: glutamine metabolism to cancer therapy. *Nat Rev Cancer.* 2016;16(10):619-634.

51. Cluntun AA, Lukey MJ, Cerione RA, Locasale JW. Glutamine metabolism in cancer: understanding the heterogeneity. *Trends Cancer.* 2017;3(3):169-180.

52. Wang X, Yang R, Zhang W, et al. Serum glutamate and glutamine-to-glutamate ratio are associated with coronary angiography defined coronary artery disease. *Nutr Metab Cardiovasc Dis.* 2022;32(1):186-194.

53. Madeira C, Alheira FV, Calcia MA, et al. Blood levels of glutamate and glutamine in recent onset and chronic schizophrenia. *Front Psych.* 2018;9:713.

54. Li X, Tu B, Zhang X, et al. Dysregulation of glutamine/glutamate metabolism in COVID-19 patients: a metabolism study in African population and mini meta-analysis. *J Med Virol.* 2022;95(1):e28150.

55. Dmitrieva-Posocco O, Wong AC, Lundgren P, et al. β-hydroxybutyrate suppresses colorectal cancer. *Nature.* 2022;605(7908):160-165.

56. Mierziak J, Burgberger M, Wojtasik W. 3-hydroxybutyrate as a metabolite and a signal molecule regulating processes of living organisms. *Biomolecules.* 2021;11(3):402.

57. Pakiet A, Kobiela J, Stepnowski P, Sledzinski T. Changes in lipids composition and metabolism in colorectal cancer: a review. *Lipids Health Dis.* 2019;18(1):29.

58. Tran NL, Lee IK, Choi J, et al. Acetate decreases PVR/CD155 expression via PI3K/AKT pathway in cancer cells. *BMB Rep*. 2021;54(8):431-436.

59. Martinez-Outschoorn UE, Peiris-Pagés M, Pestell RG, et al. Cancer metabolism: a therapeutic perspective. *Nat Rev Clin Oncol*. 2017;14(1):11-31.

60. Song Z, Wei B, Lu C, et al. Glutaminase sustains cell survival via the regulation of glycolysis and glutaminolysis in colorectal cancer. *Oncol Lett*. 2017; 14(3):3117-3123.

SUPPORTING INFORMATION

Additional supporting information can be found online in the Supporting Information section at the end of this article.